Incisor Compliance Following Operative Procedures: A Rapid 3-D Finite Element Analysis Using Micro-CT Data

Pascal Magne[a]/Derek T. Tan[b]

Purpose: New methods are available for the rapid generation of 3-D finite element models of dental structures and restorations. Validation of these methods are required. The aim of the present study is to utilize stereolithography and surface-driven automatic meshing to generate models of specific restorative conditions, and to examine these models under loading. The data generated are compared to existing experimental data in an attempt to validate the model.

Materials and Methods: An intact maxillary central incisor was digitized with a micro-CT scanner. Surface contours of enamel and dentin were fitted following tooth segmentation based on pixel density using an interactive medical image control system. Stereolithography (STL) files of enamel and dentin surfaces were then remeshed to reduce mesh density and imported in a rapid prototyping software, where Boolean operations were used to assure the interfacial mesh congruence (dentinoenamel junction) and simulate different tooth preparations (endodontic access, veneer, proximal, and Class III preparations) and restorations (Class III composites). The different parts were then imported in a finite element software package to create 3D solid models. A 50-N point load perpendicular to the tooth's long axis and centered on the incisal edge was applied either on the buccal or palatal surface. The surface strain was obtained from selected nodes corresponding to the location of the strain gauges in the validation experiments.

Results: The increase in crown flexure (compared to the unaltered tooth) ranged from near zero values (conservative endodontic access, removal of proximal enamel) to ca 10% (aggressive endodontic access, conservative Class III preparations), 23% and 34% (moderate and aggressive Class III preparations, respectively), and 91% (veneer preparation). Placement of Class III composite resin restorations resulted in 85% recovery of the original crown stiffness. 3D FEA data correlated well with existing experimental data. In two situations, smaller FEA strains were recorded compared to the experimental strains, perhaps due to enamel cracking under the strain gauges. This artefact was not simulated by the FEA models.

Conclusion: Experimental data validated the FEA models. The described method can generate detailed three-dimensional finite element models of a maxillary central incisor with different cavities and restorative materials. This method is rapid and can readily be used for other medical (and dental) applications.

Keywords: finite element analysis, anterior tooth, flexure, resin composite restoration, stiffness, veneer.

J Adhes Dent 2008; 10: 49-56. *Submitted for publication: 11.12.06; accepted for publication: 01.05.07.*

Biomedical research has inherent problems in that it can be prohibitively expensive and ethically questionable when performed on live subjects. Furthermore, certain variables cannot be monitored and measured using in vivo models. Virtual models and simulation approaches from the engineering industry, such as finite element (FE) analysis, have been utilized to overcome these barriers.[28]

FE analysis divides a large structure into a number of small, simply shaped elements. The strain and stress of these individual elements are more easily calculated than for the whole undivided structure. By solving the deformation of all the small component elements simultaneously, the deformation of the structure can be assessed. The application of a rational validation process in combination with the existing biophysical knowledge database[13] has helped refine the use of FE analysis in dental research over the last decade.[2-7,29,31] Presently, experimental-numerical approaches represent the most comprehensive in vitro investigation techniques in restorative dentistry.[29,31]

[a] *Tenured Associate Professor, Director of Esthetic Dentistry, Division of Primary Oral Health Care, School of Dentistry, University of Southern California, Los Angeles, CA, USA.*

[b] *Graduate Student, Advanced Prosthodontics, School of Dentistry, University of Southern California, Los Angeles, CA, USA.*

***Correspondence:** Dr. Pascal Magne, Oral Health Center, School of Dentistry, University of Southern California, 3151 South Hoover Street, Suite E201, Los Angeles, CA 90089-7792, USA. Tel: +1-213,740-4239, Fax: +1-213-821-5324. e-mail: magne@usc.edu*

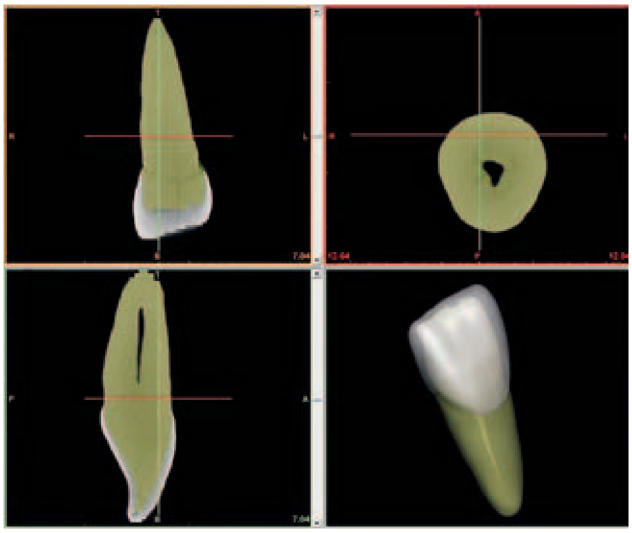

Fig 1 CT-scan data as seen in Mimics 9.0. The tooth is presented in three different cross-sectional views. Masks have been applied to enamel (white) and dentin (yellow) according to voxel density thresholding. Bottom right corner: 3-D rendering of enamel and dentin as a result of segmentation in Mimics.

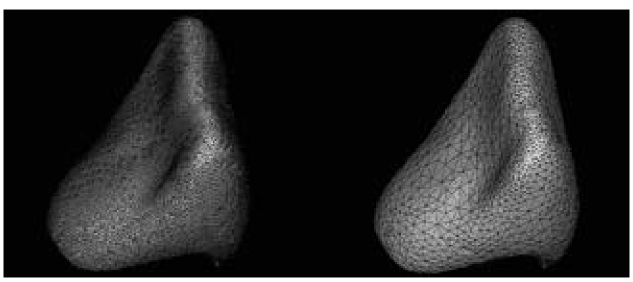

Fig 2 Left: Stereolithography triangulated (STL) file of enamel obtained through the STL+ module within Mimics. The density and quality (aspect ratio and connectivity) of the triangles is not appropriate for use in finite element analysis. Right: Enamel STL file optimized for FEA using the REMESH module within Mimics. Note the improved triangle shape and the intact geometry compared to the left-hand image in spite of a significant reduction in number of triangles.

As teeth and bones have anatomical shapes and layered structures, they cannot be assimilated to a simplified geometric representation. Sophisticated techniques have been developed to refine geometry acquisition, including the recreation and digitization of planar outlines of the spatial anatomy.[14,15] Earlier techniques resulted in the formation of meshes with less detail reproduction.[14,15] The combination of micro-CT data with FE analysis has resulted in models which are finer in texture than what could be obtained previously.[20,30] The use of stereolithography (STL) and surface-driven automatic meshing has further simplified and accelerated geometry acquisition/modification the FE modeling process.[20]

It is known that restorative procedures can make the tooth crown more deformable.[9,12,22,23] It is also recognized that there is a partial recovery of stiffness when prepared teeth are restored with conventional restorative procedures.[18,25,27] The present knowledge base has numerical data on how anterior tooth flexure is affected by various restorative conditions.[17-19]

The aim of the present study is to utilize stereolithography and surface-driven automatic meshing to generate models of specific restorative conditions, and to examine these models under loading. The data generated are compared to existing experimental data in an attempt to validate the model.

MATERIALS AND METHODS

Mesh Generation and Material Properties (Preprocessing)

A four-step procedure was followed to generate a 3-D FE model of an extracted human maxillary central incisor.[20]

First, a raw micro-CT set of slices was provided by Digisens (Ferney-Voltaire, France) with a voxel dimension of 13.67 microns. A total of 1024 slices were provided but only 75 slices (one slice out of every 14 slices) were used for the modeling.

Second, the different hard tissues visible on the scans were identified using an interactive medical image control system (Mimics 9.0, Materialise; Leuven, Belgium). Mimics imports CT and MRI data in a wide variety of formats and allows extended visualization and segmentation functions based on image density thresholding. Three-dimensional objects (enamel and dentin) are automatically created in the form of masks by growing a threshold region on the entire stack of scans. Using Mimics STL+ module, enamel and dentin were then separately converted into stereolithography files or STL, bilinear and interplane interpolation algorithms (Fig 1). Native STLs are improper for use in FEA because of the aspect ratio and connectivity of the triangles in these files. The REMESH module attached to Mimics was therefore used to automatically reduce the amount of triangles and simultaneously improve the quality of the triangles while maintaining the geometry (Fig 2). During remesh, the tolerance variation from the original data can be specified (quality of triangles does not mean tolerance variation from the original data). The quality is defined as a measure of triangle height/base ratio so that the file can be imported in the finite element analysis software package without generating any errors. The remesh operations were also applied to the dentin STL.

Third, a stereolithography handling software (MAGICS X, Materialise) was used in order to re-establish the congruence of the interfacial mesh between enamel and dentin (this congruence being lost during the previous remeshing process) using Boolean operations (addition, intersection, or subtraction of volumes). Once a congruent mesh at the dentinoenamel junction was obtained, additional Boolean operations with CAD objects were used to simulate a cylindrical fixation base (embedding the root within 2 mm of the cementoenamel junction), as well as different cavity preparations (endodontic access, Class III and veneer preparations, proximal slice) and restorations (Class III composite

Table 1 FEA geometry and characteristics for the different models

Model label	Description	Specific features	Volumetric mesh No. Elements*	Volumetric mesh No. Nodes*
NAT	Intact natural tooth (unrestored)	Central maxillary incisor	71135	15159
ENDO-CONS	Unrestored tooth with conservative endodontic access preparation	Occlusal mesiodistal width: 2.0 mm Occlusal inciso-gingival height: 3.0 mm Tapered to fit the canal apically	58839	13021
ENDO-AGGRES	Unrestored tooth with aggressive endodontic access preparation	Occlusal mesiodistal width: 4.5 mm Occlusal incisogingival height: 6.0 mm Tapered to fit the canal apically	59085	13505
VENEER PREP	Unrestored tooth with facial enamel completely removed	All facial enamel removed including mid-part of both proximal areas	60070	13345
NO-PROX	Unrestored tooth with proximal enamel completely removed	Flat proximal enamel slice (leaving dentin intact).	75138	17492
CL3-CONS	Unrestored tooth with conservative mesial and distal Class III preparations	Approx. 1.5 mm (buccolingual) x 2 mm (mesiodistal) x 6 mm (incisoginigval), soft rounded shape	47260	11321
CL3-MOD	Unrestored tooth with moderate mesial and distal Class III preparations	Approx. 2 mm (buccolingual) x 2.5 mm (mesiodistal) x 6 mm (incisoginigval), rounded shape	44334	10964
CL3-AGGRES	Unrestored tooth with aggressive mesial and distal Class III preparations	Approx. 2 mm (buccolingual) x 3 mm (mesiodistal) x 7 mm (incisoginigval), box shape	49910	11961
CL3-REST	Tooth restored with large mesial and distal Class III composites	Dimensions of restorations corresponding to CL3-AGGRES	71314	15660

*stone base excluded

resins). The exact design and dimensions of the 9 experimental conditions are described in Table 1 and can be seen in Fig 3. These specific clinically relevant situations were chosen because they reproduce existing experiments,[17-19] which will be used in the validation process of the FEA model (see Results).

Fourth, the optimized STL files of the segmented enamel and dentin parts were then imported in a finite element analysis software package (MSC.Marc/MSC.Mentat, MSC. Software; Santa Ana, CA, USA) for the generation of a volumetric mesh and attribution of material properties (Table 2). The triangulated STL files are ideal for automatic mesh generation using a tetrahedral mesher (tetrahedron elements with pyramid-like shape and 4 nodal points).

Boundary Conditions, Loadcase, and Data Processing

Fixed zero-displacement in the three spatial dimensions was assigned to the nodes at the bottom surface of the stone base and to the side opposite to the load direction (Fig 4). The tooth (enamel/dentin) and restorative materials were taken as bonded, which in group CL3-REST simulated usage of adhesive composite resin restorations. A 50-N point load was applied 1 mm from the incisal edge and centered mesiodistally on the buccal surface, except in groups VENEER PREP and NO-PROX where a palatal load was use instead. Group NAT was tested under both conditions (buccal and palatal load). The stress and strain distributions were solved using the MSC.Marc solver. As mentioned before, these specific boundary conditions, load protocol, and con-

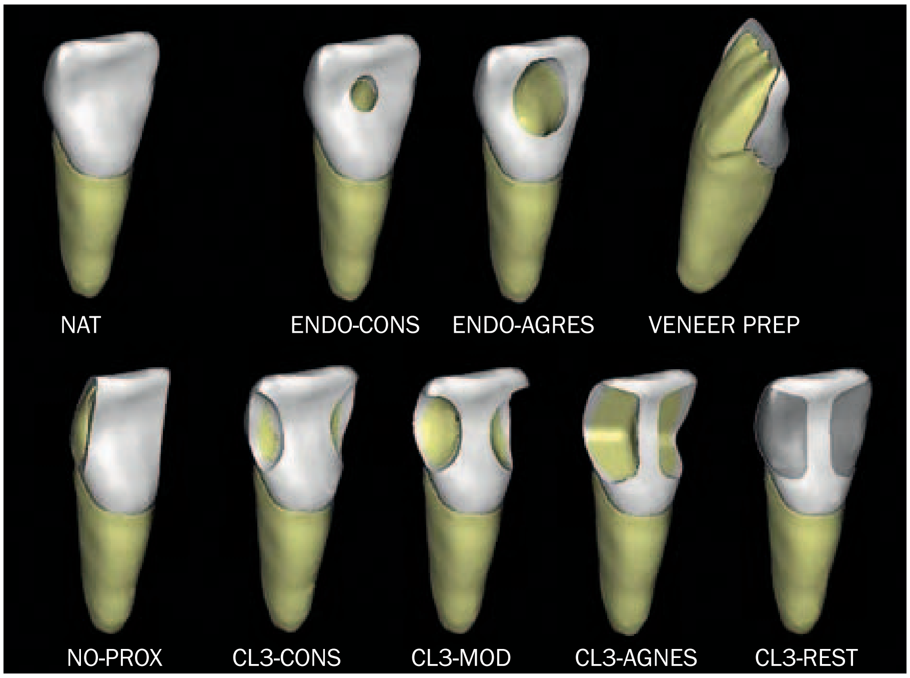

Fig 3 Congruent STL parts of enamel (white) and dentin (yellow) resulting from Boolean intersections and subtractions. The assembly of the different parts results in nine possible models (see Table 1).

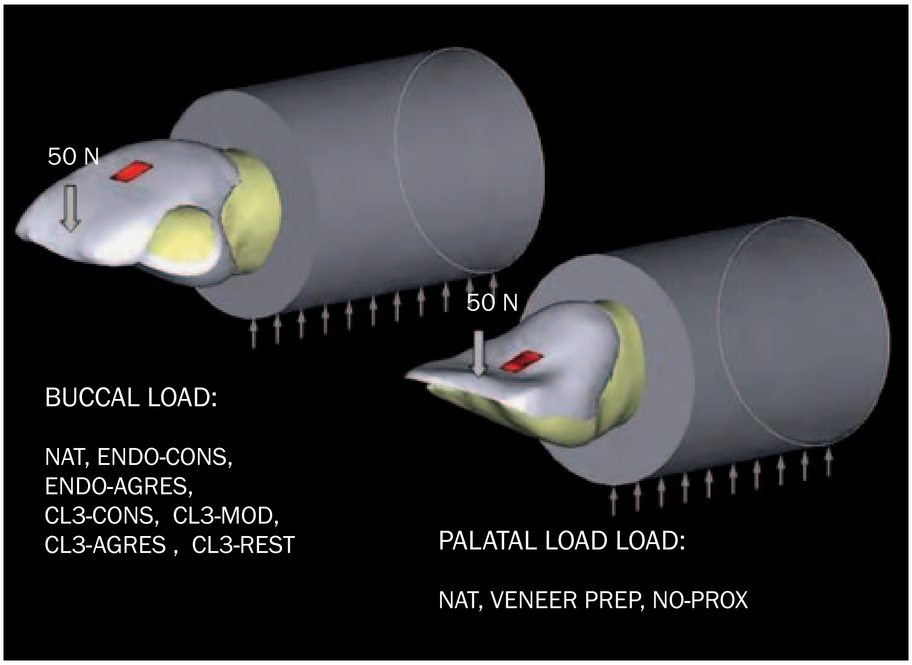

Fig 4 Load protocol and configuration, ie, a 50-N point load perpendicular to the tooth long axis and centered about 1.5 mm from the incisal edge, either on the buccal (for NAT, ENDO-CONS, ENDO-AGGRES, CL3-CONS, CL3-MOD, CL3-AGGRES, CL3-REST) or palatal surface (NAT, VENEER PREP, NO-PROX). To fit the experimental data, a cylindrical stone base (in gray) was modeled and fixed at its base (dotted circle) and along its lower outline (arrows). The surface strain was obtained from selected nodes corresponding to the location of the strain gauges in the experiment (red rectangle).

Table 2 Material properties

	Elastic modulus (GPa)	Poisson's ratio
Enamel	84.1[8]	0.30[1]
Dentin	18.6[21]	0.31[11]
Composite	10.0[10]	0.24[24]

figuration were chosen because they reproduce existing experiments.[17-19]

RESULTS

The post-processing file was accessed through MENTAT to select specific nodes on the buccal and lingual enamel at mid-height of the clinical crown and to collect the values of surface strain for each numerical model, which correspond-

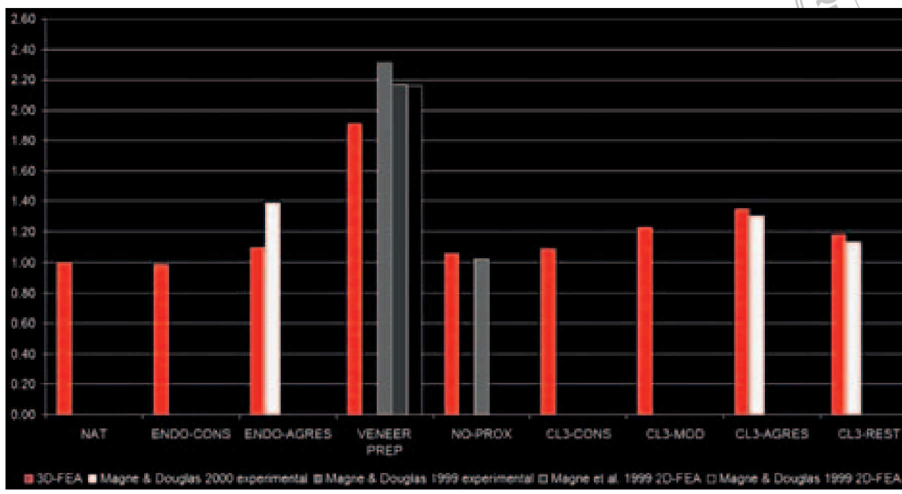

Fig 5 Results and comparison with existing experimental and numerical data.

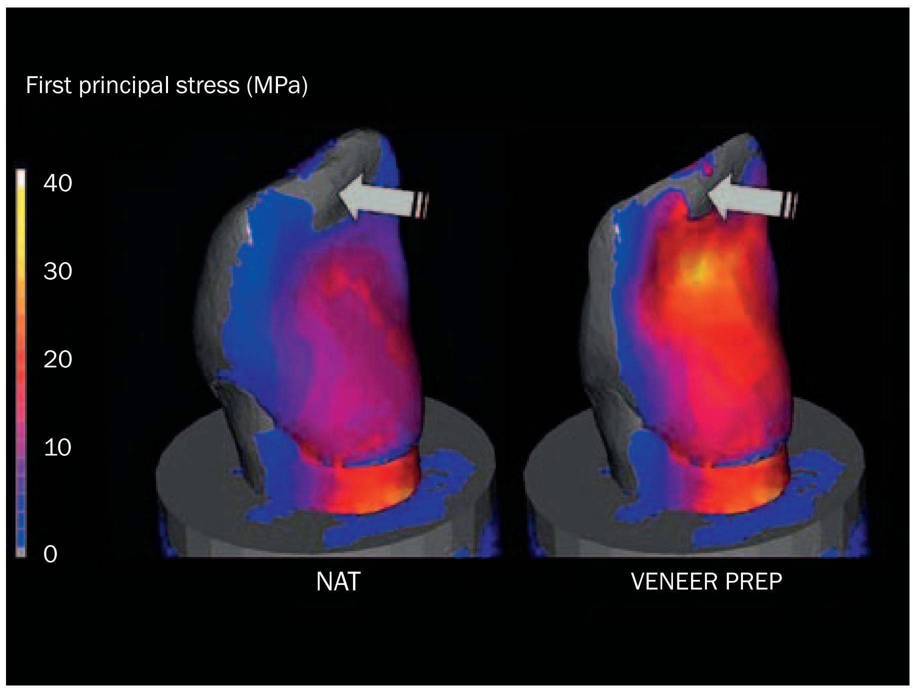

Fig 6a First principal stress distribution in models NAT and VENEER PREP. Colors = tensile stresses. Gray = compressive stresses. Note the significant increase of tensile stresses in the palatal concavity due to the loss of facial enamel. Both models behave like cantilever beams with the facial half of the tooth under compression, the palatal half under tensile stresses and a neutral plane inbetween.

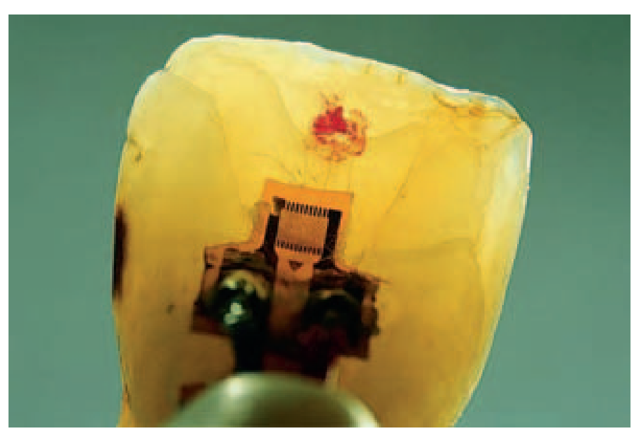

Fig 6b Sample at the end of trial (facial enamel removed) by Magne et al.[19] Multiple cracks are visible on the palatal surface. One of these has propagated mesiodistally under the strain gauge, generating an extremely intense signal compared to the FEA (cracks not modeled). Courtesy of *Journal of Prosthetic Dentistry.*

ed to the location of the strain gauges in the validation experiments. The data were transferred to a spreadsheet. For comparison between the different specimens and the existing validation experiments, normalized results were used. The absolute measurements of strain were converted to a relative value given by the following equation:

$$\text{Relative Compliance} = \frac{\text{Compliance given at a selected test conditions}}{\text{Compliance given by the unaltered tooth}}$$

$$= \frac{\dfrac{\text{maximum strain given at selected test condition}}{\text{maximum load}}}{\dfrac{\text{maximum strain given by the unaltered tooth}}{\text{maximum load}}}$$

$$= \frac{\text{maximum strain given at selected test condition}}{\text{maximum strain given by the unaltered tooth}}$$

Note that the compliance was here defined as strain/load (deformation) of the clinical crown. Results of the present simulation, along with average experimental and numerical results from existing studies[17-19] are presented in Fig 5. There is a good association between FEA and experimental values at each restorative step. A discrepancy was noted when comparing the aggressive endodontic access in the FEA to the study by Magne and Douglas,[18] 1.09 vs 1.39 of relative compliance, respectively. Another but smaller discrepancy was found when comparing the veneer preparation in the FEA to the existing studies,[17,19] 1.91 vs 2.16-2.31 of relative compliance, respectively.

DISCUSSION

A number of studies[9,12,22,23] analyzing biophysical stress and strain have shown that restorative procedures can make the tooth crown more deformable, and teeth could be strengthened by increasing their resistance to crown deformation. Because of the arrangement and position of the anterior dentition, the mechanical loads mainly act in the buccolingual plane of each tooth. Proximal contact areas restrain mesiodistal loads. The horizontal component of realistic biting loads induces bending, which is the major challenge for the incisor. The standard loadcase applied in the present analysis constitutes the most discriminating technique to study crown deformation in the anterior dentition; it also constitutes a useful validation set-up that mirrors existing experimental crown flexure measurements.

A discrepancy was observed between FEA models and the existing experiments for both models with the largest experimentally-measured strain, ie, the extensive endodontic preparation (ENDO-AGGRES) and the veneer preparation (VENEER PREP). This is not an unexpected outcome because large deformations are likely to generate enamel cracking, which, in turn, will increase the strain gauge reading during experimental testing[19] (see Fig 6b). In addition, considering that the intertooth variability reported by the existing experimental references far exceeds the FEA-experimental discrepancy, the FEA model can be considered valid. The proximal ridges were not removed by the endodontic access preparation, which limits the increase of flexibility, as shown by Reeh at al.[26] As a result, the loss of stiffness of endodontically treated teeth appears to be insignificant when the endodontic access preparation is conservative (ENDO-CONS). Thus, one must commend endodontists who are able to work through reduced access cavities, which will potentially limit the biomechanical alteration of the clinical crown and ensure a positive long-term prognosis of the restored tooth.

While the removal of proximal enamel (NO-PROX) had no significant effect on the crown compliance, the model without facial enamel (VENEER PREP) displayed the highest increase of compliance, which confirms existing experimental data showing that substantial loss of facial enamel is more likely to affect crown rigidity than is the interdental reduction of enamel or large Class III cavities.[17,18] FEA is unique in its ability to provide access to the stress distribution within hard tissues. The significant alteration generated by the veneer preparation is easily visible in Fig 6a. On the same illustration, it appears that the palatal concavity, which provides the incisor with its sharp incisal edge and cutting ability, is also an area of stress concentration and can be the nidus for crack propagation in the corresponding experimental specimen (Fig 6b).[19]

As is the case for endodontic access preparation, the extent of Class III preparations will significantly affect the compliance of the clinical crown (9% to 34% increase depending on cavity size, CL3-CONS vs CL3-AGGRES). Restoring large Class III defects with composite resin restorations will strengthen the tooth even though it does not restore the original tooth stiffness. Studies conducted by Reeh et al[25] and Reeh and Ross[27] showed a recovery of 76% to 88% in crown stiffness after the placement of composite fillings and composite veneers. In the present 3D FEA study, the restored tooth (CL3-REST) demonstrated 85% of stiffness recovery compared to the unaltered tooth, which again correlates with experimental data (86%).[18] The results obtained with the Class III and composite restored teeth are in agreement with conclusions by Douglas,[9] stating that their strength diminishes with increasing cavity size and can only approach that of the unaltered tooth in the case of small conservative cavities.

As illustrated in the present study, the proposed approach resulted in valid 3-D models with very detailed tooth anatomy and realistic computation process. Previous attempts to generate 3-D models resulted in much coarser meshes;[14.15] Verschodont et al[30] might have been the first authors to describe the development of a 3-D finite element model of a restored tooth based on a microscale CT data-acquisition technique. The tooth was scanned after being restored with a MOD composite and the 3-D geometry was obtained through the stacking of traced 2-D sections, still involving a significant amount of manual work. The approach used in the present study suggests that maximum anatomical detail is obtained by surface/interface-based meshing using stereolithography (STL) surface data. Significant advantages when using STLs are the sophisticated visualization tools (shaded wireframe 3-D views, section views, etc) and possibilities offered by the Boolean operations. The general principle of Boolean operations is that a new object can be formed by combining two 3-D objects. Objects can be united, intersected, or subtracted. When intersecting or subtracting two overlapping objects, a congruent mesh is assured at the interface between the new objects. Boolean operations with predefined CAD objects constitute an important feature. It allowed us to "digitally" simulate successive restorative procedures (Fig 3), unlike Verdonschot et al,[30] who had to "physically" prepare and restore the tooth before scanning it. In the present study, the geometry of the unaltered tooth remains, allowing for direct comparison with the different experimental conditions. One can easily foresee that the exponential development of commercial dental CT-scanners, computer processing power, and interface friendliness will make this approach even faster and more automated, allowing the rapid fabrication of patient-specific simulation of dental restorations in a very near future. Even though small differences may remain between the reality and the finite element environment, numerical modeling is able to reveal the otherwise inaccessible stress distribution within the tooth-restoration complex (Fig 6a), and it has proven to be a useful tool for facilitating the understanding of tooth biomechanics and the biomimetic approach in restorative dentistry.[16]

Although finite element analyses still have limitations, they appear to be an essential component of research and development in industry in general. Dental research, however, does not make extended use of this resource as demonstrated by the limited publication volume about numerical simulation. Geometry acquisition and three-dimensional modeling based on CT data can still be considered at a pioneering stage. Knowledge about stress distribution could have an influence on the requirements for adhesive strength. This work is an attempt to explore uncharted territories and provide inspiration as well as a method for further works in which the quality of the bond of adhesive restorations could be modeled and investigated more in detail. Therefore, minimally invasive dentistry, which is in part dependent on adhesive dentistry, should ultimately benefit from further development and research using the method of the present study.

CONCLUSION

This investigation describes a rapid method for the generation of finite element models of dental structures and restorations. Detailed three-dimensional finite element models of an incisor with different cavities and restorations were generated. A standard loadcase was applied to induce bending of the clinical crown. Surface strains were measured under the different restorative conditions and correlated with existing experimental data for model validation. Within the limitations of this study, it can be concluded that:

- 3D FEA data correlated well with existing experimental data. In two situations, smaller FEA strains were recorded compared to the experimental strains, maybe due to enamel cracking under the strain gauges. This artefact was not simulated by the FEA models.
- Endodontic preparation did not generate significant alterations of crown stiffness, especially when proximal ridges were left intact (conservative access).
- Veneer preparation (total removal of facial enamel) led to the largest increase of flexure (91%).
- Conservative and large Class III cavity preparations increased crown flexibility by 9% and 34%, respectively.
- Only 85% of the original crown stiffness could be recovered when large Class III cavities were restored with composite resin.

ACKNOWLEDGMENTS

The authors wish to express their gratitude to François Curnier (Digisens Inc., France) for providing the raw micro-CT data. This study was supported in part by MSC.Software (MSC.Marc/MSC.Mentat products) and Materialise (MIMICS/MAGICS products).

REFERENCES

1. Anusavice KJ, Hojjatie B. Influence of incisal length of ceramic and loading orientation on stress distribution in ceramic crowns. J Dent Res 1988;67:1371-1375.
2. Ausiello P, Apicella A, Davidson CL, Rengo S. 3D-finite element analyses of cusp movements in a human upper premolar, restored with adhesive resin-based composites. J Biomech 2001;34:1269-1277.
3. Ausiello P, Apicella A, Davidson CL. Effect of adhesive layer properties on stress distribution in composite restorations – a 3D finite element analysis. Dent Mater 2002;18:295-303.
4. Ausiello P, Rengo S, Davidson CL, Watts DC. Stress distributions in adhesively cemented ceramic and resin-composite Class II inlay restorations: a 3D-FEA study. Dent Mater 2004;20:862-872.
5. Cattaneo PM, Dalstra M, Frich LH. A three-dimensional finite element model from computed tomography data: a semi-automated method. Proc Inst Mech Eng [H] 2001;215:203-213.
6. Cattaneo PM, Dalstra M, Melsen B. The transfer of occlusal forces through the maxillary molars: a finite element study. Am J Orthod Dentofacial Orthop 2003;123:367-373.
7. Cattaneo PM, Dalstra M, Melsen B. The finite element method: a tool to study orthodontic tooth movement. J Dent Res 2005;84:428-433.
8. Craig RG, Peyton FA, Johnson DW. Compressive properties of enamel, dental cements, and gold. J Dent Res 1961;40:936-945.
9. Douglas WH. Methods to improve fracture resistance of teeth. In: Vanherle G, Smith DC, eds. International Symposium on posterior composite resin restorative materials. Symposium sponsored by 3M, St. Paul, MN. Peter Szulc Publishing Company (The Netherlands), 1995;433-441.
10. Eldiwany M, Powers JM, George LA. Mechanical properties of direct and postcured composites. Am J Dent 1993;6:222-224.
11. Farah JW, Craig RG, Meroueh KA. Finite element analysis of three- and four-unit bridges. J Oral Rehabil 1989;16:603-611.
12. Hood JAA. Methods to improve fracture resistance of teeth. In: Vanherle G, Smith DC (eds). International Symposium on posterior composite resin restorative materials. Symposium sponsored by 3M, St. Paul, MN. Peter Szulc Publishing Company (The Netherlands), 1995:443-450.
13. Korioth TW, Versluis A. Modeling the mechanical behavior of the jaws and their related structures by finite element (FE) analysis. Crit Rev Oral Biol Med 1997;8:90-104.
14. Lin CL, Chang CH, Ko CC. Multifactorial analysis of an MOD restored human premolar using auto-mesh finite element approach. J Oral Rehabil 2001;28:576-585.
15. Lin CL, Chang CH, Wang CH, Ko CC, Lee HE. Numerical investigation of the factors affecting interfacial stresses in an MOD restored tooth by auto-meshed finite element method. J Oral Rehabil 2001;28:517-525.

16. Magne P, Belser U. Bonded Porcelain Restorations in the Anterior Dentition – A Biomimetic Approach. Chicago: Quintessence, 2002.
17. Magne P, Douglas WH. Porcelain veneers: dentin bonding optimization and biomimetic recovery of the crown. Int J Prosthodont 1999;12:111-121.
18. Magne P, Douglas WH. Cumulative effects of successive restorative procedures on anterior crown flexure: intact versus veneered incisors. Quintessence Int 2000;31:5-18.
19. Magne P, Versluis A, Douglas WH. Rationalization of incisor shape: experimental-numerical analysis. J Prosthet Dent 1999;81:345-355.
20. Magne P. Efficient 3D finite element analysis of dental restorative procedures using micro-CT data. Dent Mater 2007;23:539-548.
21. McGuiness NJ, Wilson AN, Jones ML, Middleton J (1991). A stress analysis of the periodontal ligament under various orthodontic loadings. Eur J Orthod 1991;13:231-242.
22. Morin DL, Cross M, Voller VR, Douglas WH, DeLong R. Biophysical stress analysis of restored teeth: modeling and analysis. Dent Mater 1988;4:77-84.
23. Morin DL, Douglas WH, Cross M, DeLong R. Biophysical stress analysis of restored teeth: experimental strain measurements. Dent Mater 1988;4:41-48.
24. Nakayama WT, Hall DR, Grenoble DE, Katz JL. Elastic properties of dental resin restorative materials. J Dent Res 1974;53:1121-112.
25. Reeh ES, Douglas WH, Messer HH. Stiffness of endodontically-treated teeth related to restoration technique. J Dent Res 1989;68:1540-1544.
26. Reeh ES, Messer HH, Douglas WH. Reduction in tooth stiffness as a result of endodontic and restorative procedures. J Endod 1989;15:512-516.
27. Reeh ES, Ross GK. Tooth stifness with composite veneers : a strain gauge and finite element evaluation. Dent Mater 1994;10:247-252.
28. Satava RM. The scientific method is dead – long live the (new) scientific method. Surg Innov 2005;12:173-176.
29. Tantbirojn D, Versluis A, Pintado MR, DeLong R, Douglas WH. Tooth deformation patterns in molars after composite restoration. Dent Mater 2004;20:535-542.
30. Verdonschot N, Fennis WM, Kuijs RH, Stolk J, Kreulen CM, Creugers NH. Generation of 3-D finite element models of restored human teeth using micro-CT techniques. Int J Prosthodont 2001;14:310-315.
31. Versluis A, Tantbirojn D, Pintado MR, DeLong R, Douglas WH. Residual shrinkage stress distributions in molars after composite restoration. Dent Mater 2004;20:554-564.

Clinical relevance: Minimally invasive endodontic access and Class III preparations do not significantly alter the tooth biomechanics. Extended loss of facial enamel, as well as large Class III defects, require special attention because of the substantial loss of crown stiffness. Use of appropriate restorative methods should ensure recovery of the tooth rigidity.